A SHALLOW WATER EQUATION SOLVER AND PARTICLE TRACKING METHOD TO EVALUATE THE DEBRIS TRANSPORT

Young Seok Bang, Gil Soo Lee, and Sweng-Woong Woo

Korea Institute of Nuclear Safety

Abstract

Debris transport on the containment floor following a loss-of-coolant accident (LOCA) of the Advanced Power Reactor (APR) 1400 plant is calculated. The plant does not have a switchover to recirculation operation and, thus, requires a fully transient analysis of debris transport. To calculate the flow field in a practical computational time and reasonable accuracy, two-dimensional Shallow Water Equations are solved using the Finite Volume Method. An approximate Riemann solver, Harten-Lax-van Leer (HLL) scheme is used to capture dry-to-wet interface. To calculate the debris particle transport, a simple two-dimensional Lagrangian particle tracking model including a drag force is developed. Some efficient schemes are implemented to search a hosting cell, to determine the intersection of a particle trajectory with a cell side, and to find the reflected position of particle. The hydraulic solver is validated with an open channel flow experiment. The present model is applied to calculate the transport fraction to Hold-up Volume Tank which is a unique flow path to the containment sump of the APR1400.

1. INTRODUCTION

Debris generated by a loss-of-coolant accident (LOCA) may run all over the containment floor, block the sump screen (or strainer), increase the hydraulic head loss across the screen, and eventually, have an adverse effect on long term recirculation operation in pressurized water reactor (PWR) (Rao et al. 2003). The screen area required to incorporate the potential debris loading has been determined in terms of transport fraction (TF) defined by a ratio of amount of the debris accumulated on the screen to that generated by LOCA. For the most conventional NPP, the TF has been determined by the successive analyses on the debris distribution on containment floor before recirculation and the transport of debris after recirculation, respectively. This led to an approach to determine the TF values for blowdown phase, washdown phase, pool recirculation phase, separately. Especially, the TF during recirculation phase has been calculated by steady state analysis using computational fluid dynamic (CFD) codes, which was based on the assumption that the break flow and recirculation safety injection flow are balanced (USNRC, 2004). However, such a phase separation cannot be applied to the Advanced Power Reactor 1400 (APR1400) having no recirculation operation (KEPCO, 1997). Transport of debris to sump in the APR1400 is initiated from the early phase of a LOCA in fully transient manner.

The present study is to describe a model to predict the debris transport on the containment floor to the sump in APR1400 in a practical computational time and reasonable accuracy. For this purpose, a hydraulic model to calculate the transient flow field proposed by the present authors (Bang et al. 2009) was used. The hydraulic model for this kind of problem should be able to address the strong water jet from the break, the impingements of water jet to the structural walls, the water spreading over the floor, and the reflective waves from the walls, etc. A capability to address the complex geometry of the containment and an accurate numerical scheme to capture the sharp interface between dry floor and wet floor are also required. Practical computation time is also one of the important factors. Author's experience indicated that the use of commercial CFD code took a huge amount of computational time (~ 2 months) to get a few-seconds transient solution, as reported at the 2nd Workshop on XCFD4NRS at Grenoble (Lee at al. 2008). The present hydraulic solver is based on two-dimensional Shallow Water Equations (SWE) (Gottardi et al. 2004), the fully explicit numerical scheme and the Finite Volume Method (FVM) (Valerio et al. 2003) for the purpose of the study. The SWE solver has also been applied to the OPR1000 (Optimized Power Reactor of 1000 MWe) which have a switchover process from injection mode to recirculation mode (Bang et al[1]. 2010). Limitation due to two-dimensionality of the SWE may have an influence on the accuracy of the solution, especially, at the near-break region and the near-sump region where three-dimensional flow is dominant. In the present method, those regions are treated as a specific boundary condition which was formulated at an engineering textbook (Shames, 1962). Unstructured triangular mesh was used to simulate the complex geometry of the containment floor. For the accuracy to capture dry-to-wet interface, the Harten-Lax-van Leer (HLL) scheme (Harten at al. 1983) was adopted. An open channel flow experiment (Gottardi et al. 2004) was used to validate the present hydraulic solver. For the prediction of the debris particle transport, a particle tracking model to trace the debris particle within the calculation domain were developed, in which Lagrangian equation of motion with a drag force was solved using the pre-determined velocity field (Bang et al[2]. 2010). An efficient scheme was used to find the locations of particles on the containment floor, i.e., hosting cell determination (Martin et al. 2009). To determine the intersection of particle trajectory with a cell side and the reflected positions from the solid wall, the scheme (Haselbacher et al. 2007) was also adopted. The model is applied to calculate the transport fraction to Hold-up Volume Tank (HVT) which is a unique flow path to the containment sump in APR1400.

2. MODEL DESCRIPTION

2.1 Hydraulic Solver

The two-dimensional Shallow Water Equations (SWE) can be derived by the depth averaging process from the Navier Stokes equation and is as follows:

$$\frac{\partial \boldsymbol{W}}{\partial t}+\frac{\partial \boldsymbol{F}}{\partial x}+\frac{\partial \boldsymbol{G}}{\partial y}=\frac{\partial \boldsymbol{R}_x}{\partial x}+\frac{\partial \boldsymbol{R}_y}{\partial y}+\boldsymbol{S} \tag{1}$$

$$\boldsymbol{W}=\lfloor h, hu, hv \rfloor^T, \boldsymbol{F}=\lfloor hu, hu^2+1/2gh^2, huv \rfloor^T, \boldsymbol{G}=\lfloor hv, huv, hv^2+1/2gh^2 \rfloor^T$$

$$\boldsymbol{R}_x=\left\lfloor 0, \nu\frac{\partial hu}{\partial x}, \nu\frac{\partial hv}{\partial x}\right\rfloor^T,\ \boldsymbol{R}_y=\left\lfloor 0, \nu\frac{\partial hu}{\partial y}, \nu\frac{\partial hv}{\partial y}\right\rfloor^T \tag{2}$$

$$\boldsymbol{S}=\left\lfloor B(t),\ gh(-\frac{\partial z_b}{\partial x}-\frac{u n_m{}^2}{h^{4/3}}\sqrt{u^2+v^2}),\ gh(-\frac{\partial z_b}{\partial y}-\frac{v n_m{}^2}{h^{4/3}}\sqrt{u^2+v^2})\right\rfloor^T$$

where h, u, v, z_b, n_m, $B(t)$, and ν denote the water level from the bed, the velocity components in the x and y directions, the bed elevation, the Manning bed friction coefficient ($m^{-1/3}s$), the water source term into flow field and the dynamic viscosity, respectively. The source terms of the momentum equation include the bed slope and the friction with bed. Integrating Eq. (1) over area A surrounded by C results in

$$\int_A \frac{\partial \boldsymbol{W}}{\partial t} dA+\int_C (\boldsymbol{F}n_x+\boldsymbol{G}n_y)dC=\int_C (\boldsymbol{R_x}n_x+\boldsymbol{R_y}n_y)dC+\int_A \boldsymbol{S}dA \tag{3}$$

where n_x, n_y mean the x- and y- components of the outward unit normal vector on the surface. Assuming $\boldsymbol{W}$ to be constant within a triangle having an area A_k (Fig.1), the following can be obtained.

$$A_k\frac{d\boldsymbol{W}}{dt}+\sum_{j=1}^{3}\{\boldsymbol{F}_j n_{xj}+\boldsymbol{G}_j n_{yj}\}L_j=\sum_{j=1}^{3}\{\boldsymbol{R}_{x,j}n_{xj}+\boldsymbol{R}_{y,j}n_{xj}\}L_j+A_k\boldsymbol{S}_k \tag{4}$$

where j, L_j, n_{xj}, and n_{yj} denote the side number of the triangle, the length of side j, the components of unit normal vector in x and y direction, respectively. In Eq. (4), $\boldsymbol{W}$ are calculated at the cell center and, thus, the convective flux terms and the diffusive flux terms, $\boldsymbol{F_j}$, $\boldsymbol{G_j}$, $\boldsymbol{R_{x,j}}$, $\boldsymbol{R_{yj}}$, should be defined at each side. The new time value of $\boldsymbol{W}$ can be obtained by explicit form. In order to reserve the second order numerical accuracy in time, the predictor-corrector method (Begnudelli and Sanders, 2006) is used. In the predictor step, $\boldsymbol{W}^{n+1/2}$ are calculated by the central difference scheme for the convective flux term.

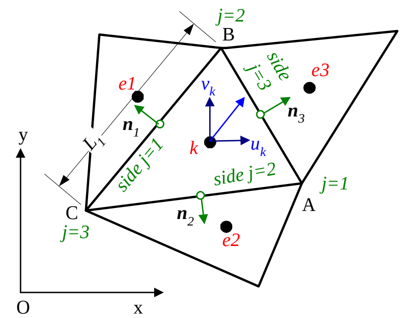

Fig. 1: Triangular cell and index notation

$$\boldsymbol{W}_k^{n+1/2} = W_k^n - \frac{\Delta t}{2A_k}\sum_{j=1}^{3}\{(\boldsymbol{F}_j^n n_{xj} + \boldsymbol{G}_j^n n_{yj}) - (\boldsymbol{R}_{x,j}^n n_{xj} + \boldsymbol{R}_{y,j}^n n_{yj})\}L_j + \boldsymbol{S}_k^{\,n}\frac{\Delta t}{2} \tag{5}$$

The corrector step calculates $\boldsymbol{W}^{n+1}$ by using an approximate Riemann solver, Harten-Lax-van Leer (HLL) scheme as follows:

$$\boldsymbol{W}_k^{n+1} = \boldsymbol{W}_k^{n+1/2} - \frac{\Delta t}{2A_k}\sum_{j=1}^{3}\{(\boldsymbol{F}_{HLL,j}^{n+1/2} n_{xj} + \boldsymbol{G}_{HLL,j}^{n+1/2} n_{yj}) - (\boldsymbol{R}_{x,j}^{n+1/2} n_{xj} + \boldsymbol{R}_{y,j}^{n+1/2} n_{yj})\}L_j + \boldsymbol{S}_k^{\,n+1/2}\frac{\Delta t}{2} \tag{6}$$

The basis for the HLL scheme is to avoid an unphysical oscillation and instability of the solution, especially at the wet-dry interface and can be described as follows:

$$\boldsymbol{F}_{HLL} = \begin{Bmatrix} \boldsymbol{F}(\boldsymbol{W}_L) & if \quad s_L > 0 \\ \boldsymbol{F}*(\boldsymbol{W}_L, \boldsymbol{W}_R) & if \quad s_L \le 0 \le s_R \\ \boldsymbol{F}(\boldsymbol{W}_R) & if \quad s_R > 0 \end{Bmatrix} \tag{7}$$

$$\boldsymbol{F}*(\boldsymbol{W}_R, \boldsymbol{W}_L) = \frac{1}{s_R - s_L}\left[(s_R \boldsymbol{F}(\boldsymbol{W}_L) - s_L \boldsymbol{F}(\boldsymbol{W}_R)) \cdot \boldsymbol{n} + s_L s_R (\boldsymbol{W}_R - \boldsymbol{W}_L)\right] \tag{8}$$

where subscripts L and R represent the values at the cell right and at the cell left to the interface, respectively. s_R and s_L are the wave speeds at those cells, as defined by following equation.

$$s_L = \min(\boldsymbol{V}_L \cdot \boldsymbol{n} - \sqrt{gh_L},\ \boldsymbol{V}*\cdot\boldsymbol{n} - c*), s_R = \max(\boldsymbol{V}_R \cdot \boldsymbol{n} - \sqrt{gh_R},\ \boldsymbol{V}*\cdot\boldsymbol{n} + c*) \tag{9}$$

where the velocity vector, $\boldsymbol{V}=u\boldsymbol{i}+v\boldsymbol{j}$, and the averaged terms ($\boldsymbol{V}*$, $c*$) are defined as follows:

$$\boldsymbol{V}*\cdot\boldsymbol{n} = \frac{1}{2}(\boldsymbol{V}_L + \boldsymbol{V}_R)\cdot\boldsymbol{n} + \sqrt{gh_L} - \sqrt{gh_R} \ , \quad c* = \frac{1}{2}(\sqrt{gh_L} + \sqrt{gh_R}) + \frac{1}{4}(\boldsymbol{V}_L - \boldsymbol{V}_R))\cdot\boldsymbol{n} \tag{10}$$

For the diffusive flux term, simple central difference scheme is used in both the predictor step and the corrector step. The derivative term of $\boldsymbol{W}$ at the side between two cells is calculated by the weighted-averaging of two derivative values determined from each cell to the common side. The turbulent viscosity was not explicitly modeled because of its small effect.

The source term of the mass equation is an addition or removal of water such as break flow or draining flow in the calculation domain, thus, it can be described by the given data. The source terms in momentum equation can be approximated by the central difference scheme and averaging process.

In order to prevent the negative water, the time step size to solve Eq's (5) and (6) should be limited level as follows (Wang and Liu, 2000):

$$\Delta t \le Min_k \left\{A_k \,/(K_{CFL} Max\left|\boldsymbol{V}\cdot\boldsymbol{n} \pm \sqrt{gh}\right|_{kj})\right\} \tag{12}$$

where K_{CFL} is a coefficient similar to the Courant-Fredrich-Lewy (CFL) number and set to 1.3 in the present study.

The boundary condition was specified as follows:

$$\begin{aligned}
&\boldsymbol{V}_j = 0, h_j = h_k && \textit{for no - slip wall} \\
&\boldsymbol{V}_j = \boldsymbol{V}_k \cdot \boldsymbol{t}_j, h_j = h_k && \textit{for slip wall} \\
&\boldsymbol{V}_j = \boldsymbol{V}_k, h_j = h_k && \textit{for open boundary}
\end{aligned} \tag{13}$$

where the subscript *j* and *k* denote the boundary side and the adjacent cell centre, respectively. $\boldsymbol{t}_j$ means the unit tangential vector to the side. Since the HVT is the vertically stepped down area, the boundary of it cannot be specified by two-dimensional approach. As an approximation to the problem, a flow rate through the boundary was specified as a function of the water level of the upstream cell. The following formula for the broad crested weir (Shames, 1962) is used.

$$u = \frac{Q_{BCW}}{hL_x}, v = \frac{Q_{BCW}}{hL_y}, \ Q_{BCW} = (\frac{2}{3})^{3/2} g^{1/2} h^{3/2} \tag{14}$$

where L_x, L_y represent the length of boundary side in *x*, *y* direction, Q_{BCW} is the flow rate, and *h* is taken from the centre of the adjacent cell.

2.2 Particle Tracking Method

Debris particle following a LOCA may be transported with colliding with other particles and settling-down due to its velocity and the gravity. The present model did not consider those aspects in the conservative viewpoint of debris transport. The position of a particle *p* at time *n+1* in two-dimensional Cartesian coordinates can be calculated as follows:

$$\boldsymbol{x}_p^{n+1} = x_p^{\ n+1} \boldsymbol{i} + y_p^{\ n+1} \boldsymbol{j} = \boldsymbol{x}_p^n + \boldsymbol{w}_p^n \Delta t_P \tag{15}$$

where the particle velocity, $\boldsymbol{w}_p = u_p \boldsymbol{i} + v_p \boldsymbol{j}$, can be obtained from the equation of motion with the fluid velocity ($\boldsymbol{V} = u\boldsymbol{i} + v\boldsymbol{j}$) which was already determined by the SWE solver.

$$m_p \frac{d\boldsymbol{w}_p}{dt} = -\boldsymbol{D}_p = -A_p C_D \frac{1}{2} \rho_f \left| \boldsymbol{w}_p - \boldsymbol{V} \right| (\boldsymbol{w}_p - \boldsymbol{V}) \tag{16}$$

Assuming the particle be in spherical shape with the diameter d_p and the density ρ_p, and express the time derivative term in explicit manner, then,

$$\boldsymbol{w}_p^n = \boldsymbol{w}_p^{n-1} - \frac{3}{4} \frac{\rho_f \Delta t_p}{\rho_p d_p} C_D^{n-1} \left| \boldsymbol{w}_p^{n-1} - \boldsymbol{V}^{n-1} \right| (\boldsymbol{w}_p^{n-1} - \boldsymbol{V}^{n-1}) \tag{17}$$

Drag coefficient, C_D can be expressed by Schiller and Neumann correlation (Krepper et al. 2008).

$$C_D = \begin{cases} 24/\mathrm{Re}_p, \ (\mathrm{Re_p} < 0.1) \\ Max\left[\frac{24}{\mathrm{Re}_p}(1 + 0.15\mathrm{Re}^{0.687}), \ 0.44 \right], \ (0.1 < \mathrm{Re_p} < 1000) \\ 0.44, \ (1000 < \mathrm{Re_p} < 1.2 \times 10^5) \end{cases} \tag{18}$$

where the particle Reynolds number is defined as follows:

$$Re_p = \frac{\rho_f \left| \boldsymbol{w}_p^n - \boldsymbol{V}^n \right| d_p}{\mu_f} \tag{19}$$

To define the fluid velocity, the cell having the particle, i.e., the hosting cell, should be identified. To save the time required to search the hosting cell, an efficient scheme (Martin et al. 2009) was introduced. If the particle is located within the cell, then the following conditions should be met (Fig. 2(a)).

$$E_1 = \boldsymbol{n_1} \cdot (\boldsymbol{p}_i - \boldsymbol{m_1}) < 0, E_2 = \boldsymbol{n}_2 \cdot (\boldsymbol{p}_i - \boldsymbol{m}_2) < 0, E_3 = \boldsymbol{n}_3 \cdot (\boldsymbol{p}_i - \boldsymbol{m}_3) < 0 \tag{20}$$

where $\boldsymbol{m_1}$, $\boldsymbol{m_2}$, $\boldsymbol{m_3}$, and $\boldsymbol{n_1}$, $\boldsymbol{n_2}$, $\boldsymbol{n_3}$ denote the vectors to the centre and the unit normal vectors of three side of the triangle and $\boldsymbol{p}_i$ is a particle position vector, respectively. If those conditions are not met, the adjacent cell sharing the side *j* with the cell *k* and having the maximum of E_j will be searched first.

An intersection of a particle trajectory with the side of a cell can be determined (Fig.2) (Haselbacher et al. 2007). Consider the particle moves from the position $\boldsymbol{p}$ to the position $\boldsymbol{q}$ with intersecting with the side at the position $\boldsymbol{r}$. Assuming $\boldsymbol{t}$ is the unit vector from $\boldsymbol{p}$ to $\boldsymbol{q}$, $\boldsymbol{C}$ is a centre of the side, and vector $\boldsymbol{r}$-$\boldsymbol{p}$ $=\alpha\boldsymbol{t}$, then

$$(\boldsymbol{r}(\alpha) - \boldsymbol{C}) \cdot \boldsymbol{n} = 0 \tag{21}$$

From those equations, α can be determined as follows:

$$\alpha = \frac{(\boldsymbol{C} - \boldsymbol{p}) \cdot \boldsymbol{n}}{(\boldsymbol{t} \cdot \boldsymbol{n})} \tag{22}$$

Let the distance from $\boldsymbol{p}$ to $\boldsymbol{q}$ be d, $\alpha > d$ means the position $\boldsymbol{q}$ is inside the cell. If the intersecting side is a reflective boundary, i.e., solid wall, the reflection of the particle should be considered (Fig.3) (Haselbacher et al. 2007). From the vector operation, the new position $\boldsymbol{q}'$ can be determined as follows:

$$\boldsymbol{q}' = \boldsymbol{q} - 2\{(\boldsymbol{q} - \boldsymbol{r}) \cdot \boldsymbol{n}\}\boldsymbol{n} \tag{25}$$

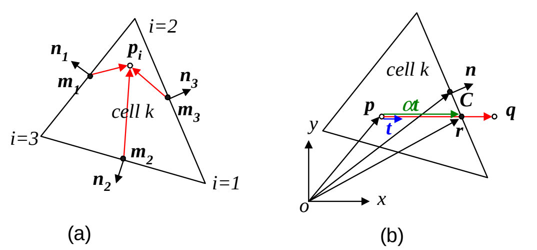

Fig. 2: Hosting cell criteria and intersection with particle trajectory

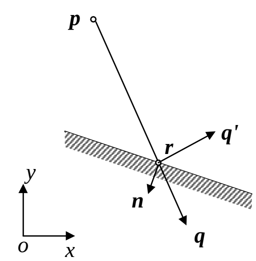

Fig. 3: Treatment of reflected boundary

3. MODEL VALIDATION

The present hydraulic model was validated with the open channel experiment cited in the reference (Gottardi et al. 2004). Fig. 4 shows a schematic representation of the experiment. The reservoir was 2.4×2.4m rectangular shape and was initially filled with water to a height of 0.2m. An L-shaped open channel was connected to the reservoir and was in a dry state. A gate in front of the pool was instantaneously ruptured and the water was discharged into the channel. Water level was measured at several locations as in Fig. 4. The experiment was considered to be similar to the flow behavior around the structural wall at the containment floor. The computational mesh was prepared as shown in Fig. 4. Total number of cell was 1238. At the exit of the channel, the open boundary condition was imposed while no-slip condition at all wall boundaries. The calculated water level at the point P3 is shown in Fig. 5, compared with the experimental data. The calculated behavior was reasonably agreed to the measured one. Especially the time of change from dry to wet at the point was well-predicted and the surface wave reflected from the wall was also reasonably simulated. The uncertainty of the measurement was not available from the reference. A deviation after 10 seconds from the experiment data was due to the difference in the measured point and the calculated one and to the modeling of the gate. The difference may be attributed to the lack of turbulence model and the limitation of SW equations. However, it is believed that the physical phenomena in the open channel can be reasonably predicted within a practical accuracy. Also the improvement of the modeling scheme may minimize the difference.

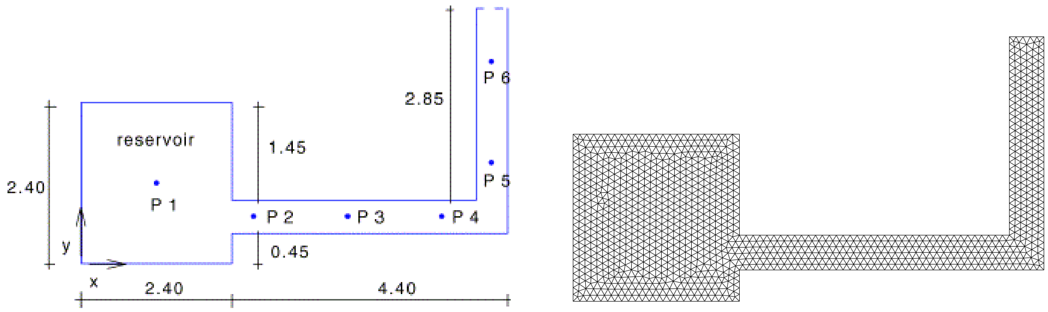

Fig. 4: Experiment setup and computational mesh

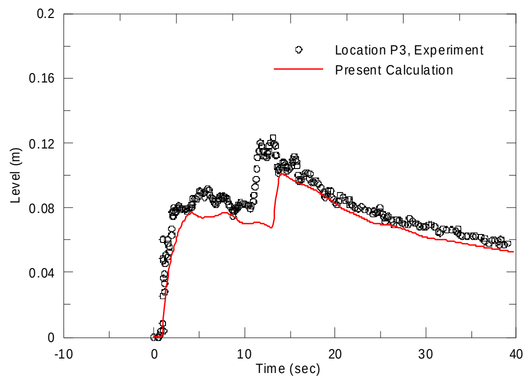

Fig. 5: Comparison of water level

4. PLANT CALCULATION

A transient flow field on containment floor following a large break LOCA of APR1400 was calculated. Fig. 6 shows a computational domain which has an annulus region between the containment inner wall (CIW) and the secondary shield wall (SSW), two D-shaped regions between the SSW and the primary shield wall (PSW). Structures simulating the steam generator (SG) pedestals and the reactor coolant pump (RCP) pedestals were also included. In the right-hand-side of the domain, the HVT was surrounded by three pieces of structures such that four entrances to HVT are available. In the left-hand-side, the structural walls of two compartments were the boundaries for the domain. Total number of cells and nodes were 7228 and 4245, respectively.

Double ended hot leg guillotine break LOCA of the APR1400 was simulated and the time-dependent break flow rate was adopted from the APR1400 Safety Analysis Report (KEPCO 1997). The calculation was conducted to 100 seconds. Fig. 7 shows the calculated water levels and velocity vectors over the domain at 5 seconds and 10 seconds after LOCA, respectively. The region without velocity vector denotes the region in a dry state. From the comparison between two figures, the water spreading behavior and the related wave propagation both inside and outside SSW can be observed. The computational time was 11032 CPU seconds (3.02 hours) in Pentium IV 3.4 GHz processor, which clearly indicated that the calculation can be done in a practical computational time.

The particle tracking calculation was conducted for the particle having a diameter of 0.02m and a density and 900kg/m^3. It was assumed that the particles were distributed randomly within the circle whose center and radius are (0, 6.5151m) and 0.9m, respectively (a region between the PSW and the SG pedestal in upper region). Particles were inserted to the circle such that the number of particle decreased linearly from 98 to 2 during 9.5 seconds, which resulted in 1000 particles in total. It was based on that behavior of the debris generation was similar to one of break flow. It was found that an instantaneous insertion of all particles at zero second resulted in less number of particles entering the HVT. Due to the initially high fluid velocity, the particles move far from the HVT entrance 1. The calculation time step was 0.001~0.01 seconds which was selected for the given velocity field.

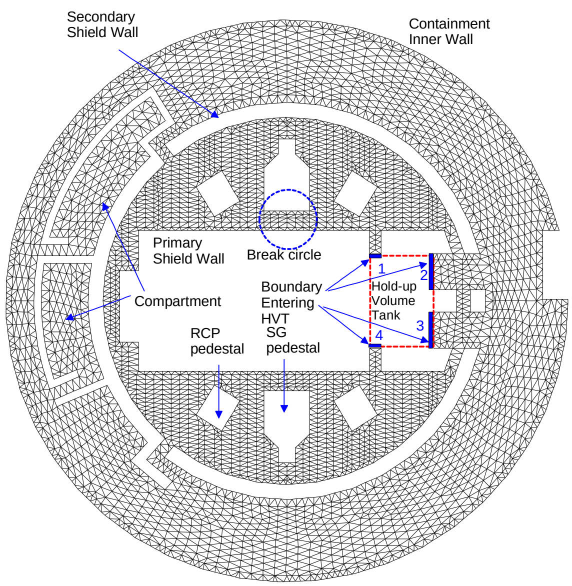

Fig. 6: Calculation domain for APR1400 containment

Fig. 8 shows the calculated particle trajectories at 5 and 10 seconds. Two figures indicated a few particles reached the HVT in 10 seconds. The reason for the low transport until 10 seconds was the high velocities of particles near the entrance 1. As time progressed, the particles with relatively low velocities were entrained by fluid stream to HVT entrance 1. Fig. 9 shows the number of particles entering the HVT. It increased significantly after 10 seconds. For the case of density 900kg/m^3, 120 out of 1000 particles were transported until 100 seconds.

To confirm the reliability on 1000 particles, additional calculations were conducted for the different number of particles. Fig. 10 shows the result from those calculations, which implied that the convergence can be guaranteed by increasing the total number of particle and the TF calculated from 1000 particles can be credited within 10^{-2} level (0.12 at 1000 particles vs. 0.126 at 2000 particles).

To understand the effect of particle density on transport, additional calculations were conducted for the particle densities ranging from 400 to 1300 kg/cm^3 and having the size of 0.02 m. Fig. 9 compares the results of calculations for different densities. It can be shown the lower particle density led the more particles to the HVT. The calculated TF was 0.164 for the case of 400 kg/cm^3.

To evaluate the effect of particle size on transport, additional calculations were conducted for the particle sizes 0.002, 0.01 and 0.05 m and the density of 900 kg/cm^3. Fig. 11 shows the comparison of the results for different sizes. The comparison shows a clear trend the smaller size the more particles to the HVT. The calculated TF was 0.213 for 0.002 m case. The reason for that trend was a drag force to particle with respect to the particle size.

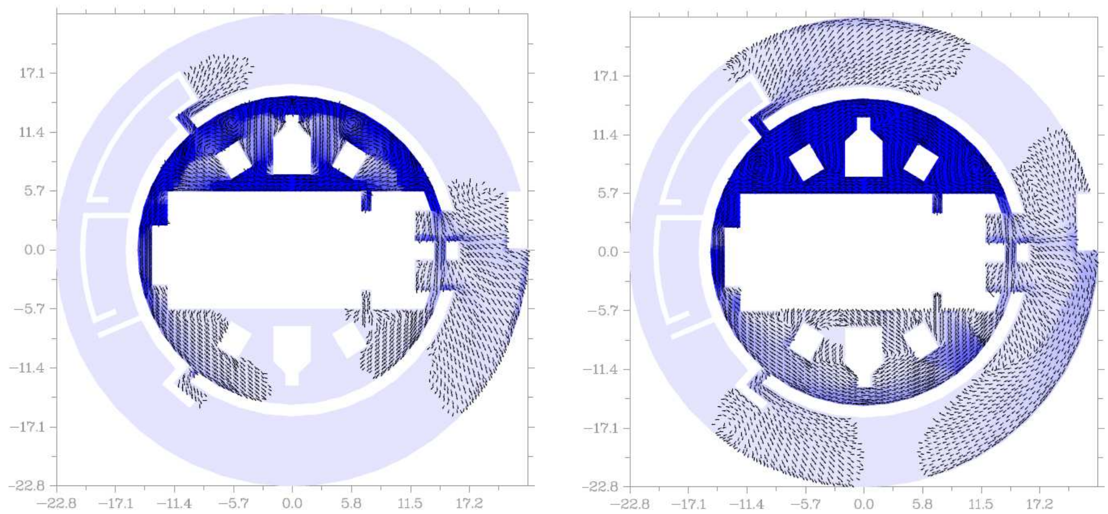

(a) t=5 sec (b) t=10 sec

Fig. 7: Result of flow field calculation

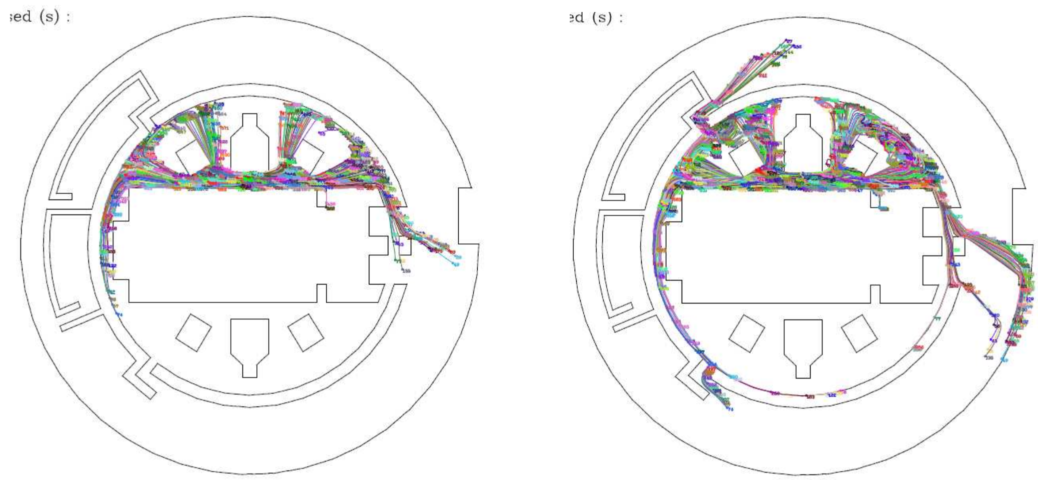

(a) t=5 sec (b) t=10 sec

Fig. 8: Result of debris particle tracking

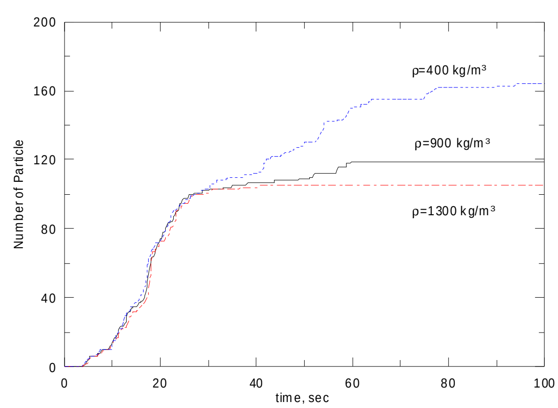

Fig. 9: Comparison of number of particles in HVT (effect of density)

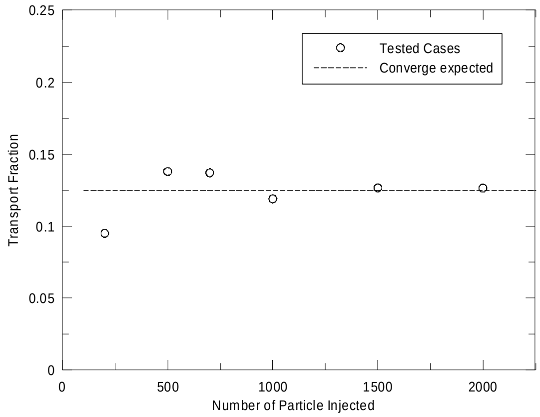

Fig. 10: Convergence of transport fraction with number of particles

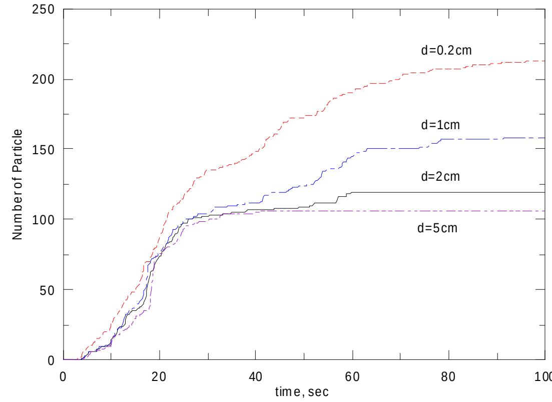

Fig. 11: Comparison of number of particles in HVT (effect of size)

5. CONCLUSIONS

Debris transport on the containment floor following a LOCA was calculated for the APR1400 plant which does not have a switchover to recirculation operation. Two-dimensional Shallow Water Equations were solved to get a transient flow field within a practical computational time and reasonable accuracy. The Finite Volume Method was used with Harten-Lax-van Leer scheme to capture dry-to-wet interface. For the debris particle transport, a simple two-dimensional Lagrangian particle tracking model including a drag force is developed. Advanced schemes to search a hosting cell, to determine the intersection of particle trajectory with a cell side, and to find the reflected position of particle were implemented. The hydraulic solver was validated with an open channel experiment, which indicated that the transient flow field could be predicted within a reasonable accuracy. The present model was applied to calculate the transport fraction to Hold-up Volume Tank. As a result, the debris transport through the containment floor to HVT was calculated within a practical computational time and the predicted transport fraction until 100 seconds was 13~22 % for the particle density range of 400~1300 kg/m^3 and for the particle diameter range of 0.002~0.05 m.

.

REFERENCES

Bang et al. "Prediction of free surface flow on Containment floor using a Shallow Water Equation Solver", *Nuclear Engineering and Technology*, Vol.41, No.8, 1045-1052 (2009).

Bang et al.[1] "Distribution and Transport of Debris Particles on Containment Floor During Blowdown and Recirculation", *Proceedings of the European Nuclear Conference 2010*, Barcelona, Spain, May 30~July 2, 2010.

Bang et al. [2] "A Particle Tracking Model to Predict the Debris Transport on the Containment Floor", *Nuclear Engineering and Technology*, Vol.42, No.2, 241-248 (2010).

Begnudelli L. and Sanders B.F., "Unstructured Grid Finite-Volume Algorithm for Shallow-Water Flow and Scalar Transport with Wetting and Drying", *ASCE Journal of Hydraulic Engineering*, Vol.132, 371-384. (2006).

Gottardi G., et al., "Central Scheme for Two-Dimensional Dam-break Flow Simulation", *Advances in Water Resources*, Vol.27, 259-268 (2004).

Harten A., Lax P. D., and van Leer B., "On Upstream Differencing and Godunov-type Schemes for Hyperbolic Conservation Laws", *SIAM Review*, Vol.25, No.1, 35-61 (1983).

Haselbacher, A., et al., "An Efficient and Robust Particle-Localization Algorithm for Unstructured Grids", *Journal of Computational Physics*, Vol.225, 2198–2213 (2007).

KEPCO, *Standard Safety Analysis Report of Korean Next Generation Reactors 1400*, KEPCO, Seoul, Korea, 1997.

Krepper E., et al., “Numerical and Experimental Investigations for Insulation Particle Transport Phenomena in Water Flow”, *Annals of Nuclear Energy*, Vol.35, 1564-1579 (2008).

Lee J. I., et al., “Debris Transport Analysis Related with GSI-191 in Advanced Pressurized Water Reactor Equipped with In-containment Refueling Water Storage Tank”, *Proceedings of Experiment and Computational Fluid Dynamics for Nuclear Reactor Safety (XCFD4NRS)*, Grenoble, France, Sep.10~12, (2008).

Martin, G.D., et al., “Particle Host Cell Determination in Unstructured Grids”, *Computers and Fluids*, Vol.38, 101–110 (2009).

Rao, D.V., et al, *Knowledge Base for the Effect of Debris on Pressurized Water Reactor Emergency Core Cooling Sump Performance*, NUREG/CR-6808, USNRC, Washington, DC., USA, 2003.

Shames I.H., *Mechanics of Fluids*, McGraw-Hill, New York, USA, 1962.

USNRC, *Safety Evaluation by the Office of Nuclear Reactor Regulation Related to NRC Generic Letter 2004-02, Nuclear Energy Institute Guidance Report (Proposed Document Number NEI 04-07), “Pressurized Water Reactor Sump Performance Evaluation Methodology*, USNRC, Washington D.C., USA, 2004.

Valerio C., et al., “Finite Volume Method for Simulating Extreme Flood Events in Natural Channels”, *Journal of Hydraulic Research*, Vol.41, No.2, 167-177, (2003).

Wang J.W. and Liu R.X., “A Comparative Study of Finite Volume Methods on Unstructured Meshes for Simulation of 2D Shallow Water Wave Problems”, *Mathematics and Computers in Simulation*, Vol.53, 171–184. (2000).